

# Optimal Aircraft Path Planning in a Structured Airspace Using Ensemble Weather Forecasts

Antonio Franco, Damián Rivas, and Alfonso Valenzuela  
Department of Aerospace Engineering  
Escuela Técnica Superior de Ingeniería, Universidad de Sevilla  
Seville, Spain  
antfranco@us.es, drivas@us.es, avalenzuela@us.es

**Abstract**— The optimisation of the aircraft route taking into account wind and temperature uncertainties is addressed in this work. These uncertainties are obtained from ensemble weather forecasts. A structured airspace is considered, which is defined by a set of waypoints and a set of allowed connections between each pair of waypoints. The analysis is focused on a cruise flight composed of several segments connecting given waypoints. The optimal route is seen as a path in a graph. The optimal path is obtained by applying a Mixed-Integer Linear Programming algorithm. The objective is to perform a trade-off between efficiency (minimum average flight time) and predictability (minimum dispersion of the flight time). Results are presented for a given trans-oceanic route, considering a real ensemble weather forecast.

**Keywords**- probabilistic trajectory optimisation; weather uncertainty; ensemble weather forecasting

## I. INTRODUCTION

From the operational point of view, trajectory optimisation is a subject of great importance in Air Traffic Management (ATM). It aims at defining optimal flight procedures for a given aircraft mission that lead to cost-efficient flights. Aircraft trajectory optimisation is an important tool to improve the efficiency of operations and, therefore, it contributes to enhance the efficiency of the ATM system.

A promising approach to improve the ATM system performance while maintaining high safety standards is to integrate uncertainty information. Among the various uncertainty sources that affect the ATM system, weather has perhaps the greatest impact. In particular, weather uncertainty has an important impact on the route planning process. Nilim et al. [1] develop a dynamic routing strategy for the en-route portion of flights subject to adverse weather; they minimise delays modelling the weather processes as stationary Markov chains. Grabbe et al. [2] design a sequential optimisation method for traffic flow management, accounting for imperfect weather information, with strategic and tactical control loops; at the tactical level, weather-avoidance rerouting is implemented using a deterministic Dijkstra's algorithm. Sauer et al. [3] analyse the uncertainty related to the displacement and growth of thunderstorm nowcasts to enhance an adverse weather avoidance model for aircraft routing.

In this paper, the optimisation of the aircraft route taking into account wind and temperature uncertainties is addressed; adverse weather phenomena are not considered. The wind and the temperature uncertainties are obtained from ensemble weather forecasts, and the analysis is focused on the cruise flight. Girardet et al. [4] propose an algorithm for optimal path planning in the presence of a deterministic, static wind field, and develop an adaptation to spherical coordinates, especially suitable for long flights. The algorithm is applied to provide minimum-time trajectories, considering a kinematic model for the aircraft motion. An analysis of wind-optimal cruise trajectories using ensemble probabilistic forecasts together with a robust optimal control method is performed in Gonzalez-Arribas et al. [5]; the objective is to provide free-flight trajectories that minimise a linear combination of the mean flight time, the mean fuel consumption and the difference between the maximum and the minimum values of the flight time; a dynamic model for the aircraft motion is considered, with a variable airspeed; the wind field considered for the case study is static, although the authors claim that the methodology is applicable to time-dependent wind fields. As a free-flight environment is far from being a reality, Rosenow et al. [6] develop an algorithm to adapt optimal free-route trajectories to the current navais infrastructure. By applying filtering and smoothing processes to the waypoints and airways, the authors come up with an adapted trajectory, which is claimed to be efficient for being close to the free-flight optimal one.

The main objective of this work is to develop a methodology capable of finding stochastic optimal paths, within a structured airspace, in presence of uncertain winds and uncertain air temperatures. The wind and temperature fields are provided by an ensemble weather forecast, which is obtained for an intermediate lead time between departure and arrival. As in [5], both the mean flight time and the difference between the maximum and the minimum values of the flight time are included in the objective function; however the main contribution with respect to [5] and [6] is the explicit consideration of a structured airspace, which is a more appropriate assumption not only for the traditional air route network, but also for the new free-route airspace concept, because both make use of predefined waypoints.

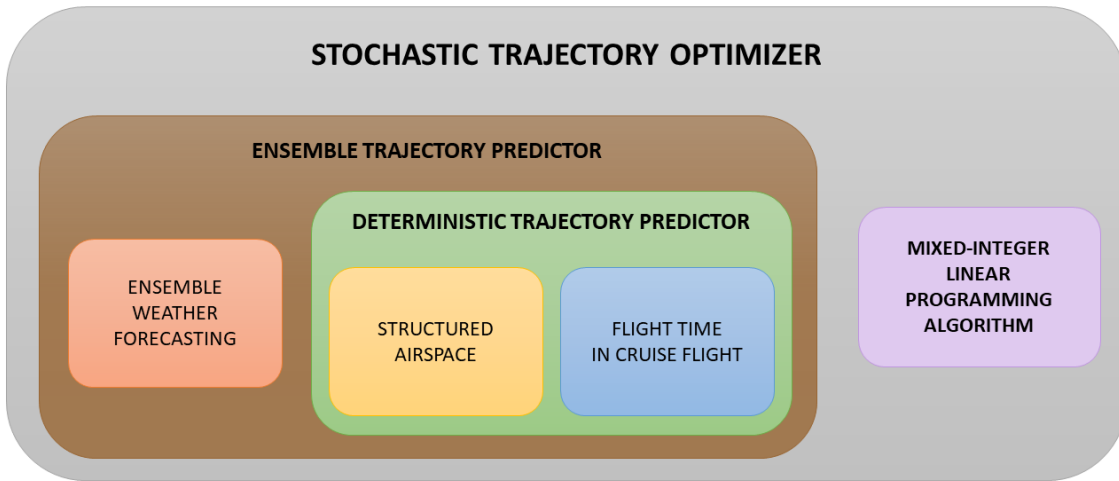


Figure 1. Methodology proposed for optimal path planning.

## II. PROBLEM FORMULATION AND METHODOLOGY

In this Section, the optimisation of the aircraft route taking into account weather uncertainty is formulated, and the resolution methodology is explained. In particular, a stochastic trajectory optimiser has been developed, composed of several blocks depicted in Fig. 1.

First, ensemble weather forecasting is addressed in Section II.A, as it is the way used in this work to quantify wind and temperature uncertainties. Second, as the analysis is focused on the cruise flight, the airspace structure considered is described in Section II.B, and the procedure to obtain the flight time is developed in Section II.C; the resulting equations are the base of a deterministic trajectory predictor. Then, the ensemble trajectory prediction approach is explained in Section II.D. Finally, the methodology proposed for stochastic optimal path planning is described in Section II.E.

### A. Ensemble weather forecasting

To model weather for strategic planning horizons, a probabilistic approach is the appropriate one, so that the inherent weather uncertainty can be taken into account. The use of probability forecasts is currently encouraged by meteorologists. For instance, the American Meteorological Society [7] recommends to substantially increase the use of probability forecasts, because they enable users to make decisions based on quantified weather uncertainty, what would lead to socio-economic benefits.

Today's trend is to use Ensemble Prediction Systems (EPS), which attempt to characterise and quantify the inherent prediction uncertainty based on ensemble modelling. Ensemble forecasting is a prediction technique that consists in running an ensemble of weather forecasts by slightly altering the initial conditions and/or the parameters that model the atmospheric

physical processes, and/or by considering time-lagged or multi-model approaches (Arribas et al. [8]; Lu et al. [9]). Thus the EPS generated by this technique is a representative sample of the possible (deterministic) realisations of the potential weather outcome, as indicated by Steiner et al. [10].

An ensemble forecast is a collection of typically 10 to 50 weather forecasts (referred to as members). Cheung et al. [11] review various EPSs: PEARP (from Météo France), consisting of 35 members; MOGREPS (from the UK Met Office), with 12 members; the European ECMWF, with 51 members; and a multi-model ensemble (SUPER) constructed by combining the previous three forming a 98-member ensemble. Some examples of EPS from the US are MEPS (from the Air Force Weather Agency) with 10 members, and SREF (from the National Centers for Environmental Prediction) comprised of 21 members.

Ensemble forecasting has proved to be an effective way to quantify weather prediction uncertainty. The uncertainty information is on the spread of the solutions in the ensemble, and the hope is that this spread bracket the true weather outcome [10]. It is important to notice that for strategic planning the analysis of all the individual ensemble members must be included (rather than an ensemble mean), as remarked by Steiner et al. [12].

### B. Airspace structure

In optimal path planning, the aircraft can be considered to be flying within a free-flight airspace or within a structured airspace. On the one hand, in a free-flight airspace, an airspace user can freely plan a route going through any point between the origin and the destination. On the other hand, a structured airspace is defined by a set of waypoints and a set of allowed connections between each pair of waypoints, referred to as airways.

Dancila and Botez [13] address the selection of the geographical area within which the optimisation algorithm has to find the best route. They assert that it is an important issue in aircraft trajectory optimisation, because it affects both the optimality of the solution found and the computational efficiency of the algorithm. From the point of view of optimality, large searching areas are preferred, because it is not known in advance how far away from the great circle the weather will drift the optimal trajectory; on the other hand, from the computational effort point of view, small searching areas are advisable. Therefore, a trade-off between optimality and computational efficiency has to be reached. In particular, the authors propose an elliptical-like area, with the departure and destination airports not necessarily at the foci.

In this work, a structured airspace is considered. The geographical area and the routing grid are defined based on [13], with slight modifications. In particular, the following procedure is applied.

- First, a regular grid of waypoints is defined in the weather forecast retrieval area, with a step  $\delta_{lat}$  in latitude and  $\delta_{lon}$  in longitude. This area goes from  $\phi_{min}$  to  $\phi_{max}$  in latitude, and from  $\lambda_{min}$  to  $\lambda_{max}$  in longitude.
- Then, the geographical search area is restricted to be inside a spherical ellipse with foci located at arrival and destination airports, and with major axis equal to  $(1+k)r_{gc}$ , where  $r_{gc}$  is the great circle distance between the departure and destination airports, and  $k$  is a tuning parameter that controls the extension of the search area. Hence, the waypoints whose sum of orthodromic

distances to the departure airport and to the destination airport is greater than  $(1+k)r_{gc}$  are discarded. An example of the searching area for a Madrid-Mexico flight with  $k = 0.04$  and  $\delta_{lat} = \delta_{lon} = 1^\circ$  is shown in Fig. 2; the great circle trajectory between the origin and the destination is also represented as a reference.

Furthermore, each waypoint inside the search area is connected to some of its neighbours in a  $7 \times 7$ -waypoint square centred at the waypoint of interest, provided that the neighbours are inside the search area as well. A sketch of the connections of a waypoint is depicted in Fig. 3; the waypoint of interest is represented as a solid triangle; the neighbours to which it is connected are depicted as solid squares, whereas the neighbours to which it is not connected are depicted as circumferences.

Finally, the arrival and destination airports are considered to be connected to those surrounding waypoints with a difference in latitude of less than  $2\delta_{lat}$  and a difference in longitude of less than  $2\delta_{lon}$ , provided that those waypoints are inside the search area. The scheme of connections considered provides a great flexibility to the aircraft route, because it allows for a large variety of courses and segment lengths.

Note that this approach can be adapted to the current Air Traffic Services route network; in that case, the set of waypoints (which may be based on the nav aids location) and the airways would be given, thus replacing the uniform grid previously presented. The consideration of an elliptical-like restricted geographical search area would still be beneficial.

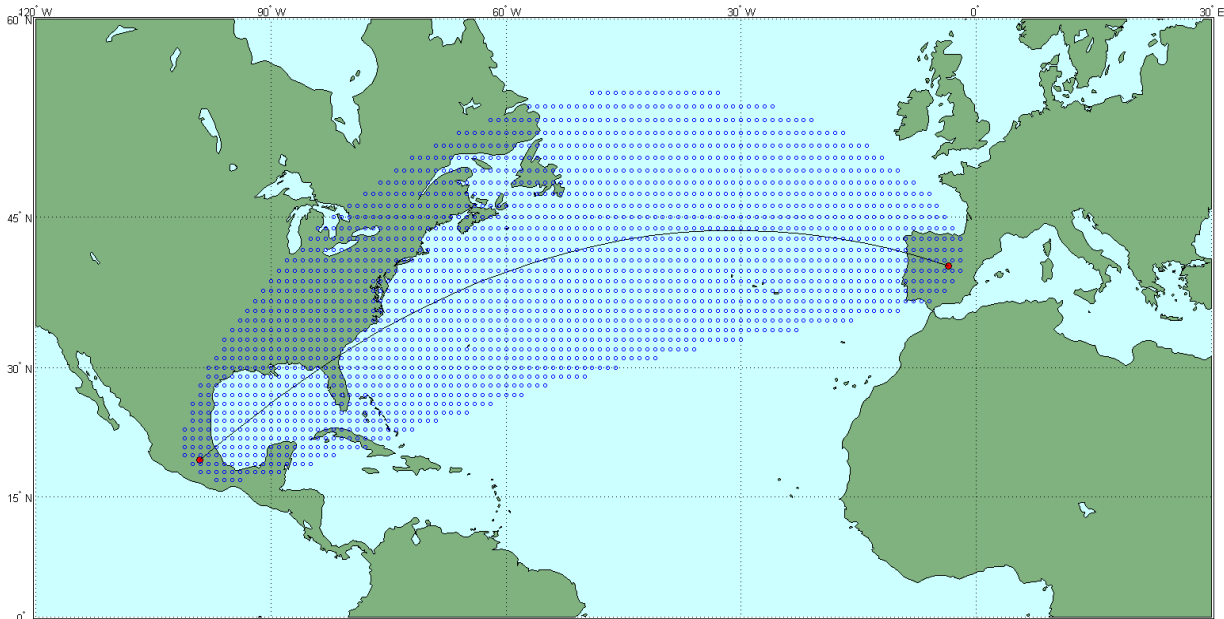


Figure 2. Search area and waypoint grid. Origin and destination airports (red dots); waypoints (blue circles); great circle trajectory (black solid line).

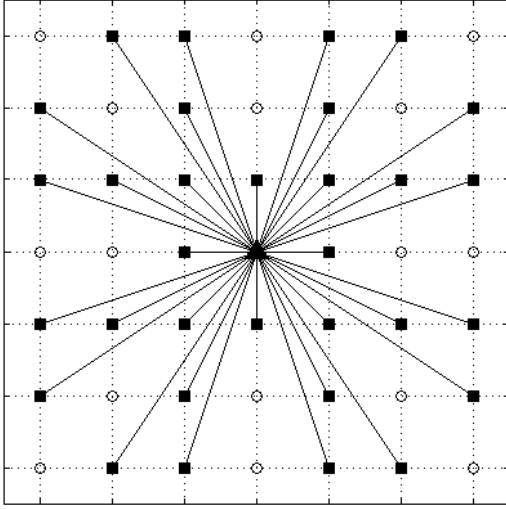


Figure 3. Sketch of connections of a waypoint. Waypoint (black filled triangle); connections (black segments); connected neighbours (black filled squares); not connected neighbours (black circumferences).

### C. Flight time in cruise flight

As already indicated, in this paper the flight time in cruise flight is studied. In accordance with the airspace structure defined in Section II.B, the cruise is considered to be formed by  $p$  cruise segments, each one of them defined by a constant course, and flown at constant Mach number and constant pressure-altitude, as required by Air Traffic Control (ATC) practices. The Earth is assumed to be spherical, with mean radius  $R_E = 6371$  km. Time-invariant wind and temperature fields are considered, which are provided by an EPS obtained for an intermediate lead time between departure and arrival. In this work, constant pressure altitude is assumed to coincide with constant geopotential altitude,  $h$ ; although this may not be true for a non-standard atmosphere, this is a common assumption in aircraft path planning (see, for instance, [4] and [5]), as the equations of motion correspond to a horizontal cruise flight.

Let the longitude and latitude of the waypoints that define the cruise segment  $j$  be denoted as  $\lambda_{j-1}$ ,  $\lambda_j$ ,  $\phi_{j-1}$ , and  $\phi_j$ , respectively. Then, the course  $\psi_j$  and the segment length  $(r_f)_j$  can be computed from the navigation equations, as follows

$$\tan \psi_j = \frac{\lambda_{j-1} - \lambda_j}{\ln \left[ \frac{\tan(\pi/4 - \phi_{j-1}/2)}{\tan(\pi/4 - \phi_j/2)} \right]}, \quad (1)$$

$$(r_f)_j = \begin{cases} \frac{(R_E + h)(\phi_j - \phi_{j-1})}{\cos \psi_j}, & \text{if } \phi_j \neq \phi_{j-1} \\ (R_E + h) \cos \phi_{j-1} |\lambda_j - \lambda_{j-1}|, & \text{if } \phi_j = \phi_{j-1} \end{cases} \quad (2)$$

Sketches of a multi-segment cruise and a generic cruise segment can be found in Fig. 4 and Fig. 5, respectively. In cruise segment  $j$ , the flight is subject to along-track winds,  $w_{AT_j}(r)$ , crosswinds,  $w_{XT_j}(r)$ , and a non-standard air temperature  $T(r)$ , which vary along the cruise ( $r$  represents the distance flown by the aircraft). The effects of the crosswinds are analysed by taking them into account in the kinematic equations, ignoring the lateral dynamics, and translating the crosswind into an equivalent headwind. This leads to a reduced ground speed, which for cruise segment  $j$  is given by

$$V_{g_j}(r) = \sqrt{M^2 \kappa R_g T(r) - w_{XT_j}^2(r) + w_{AT_j}(r)}, \quad (3)$$

where  $\kappa = 1.4$  is ratio of specific heats of the air,  $R_g = 287.053$  J/(kg K) is the gas constant of the air, and  $M$  is the Mach number.

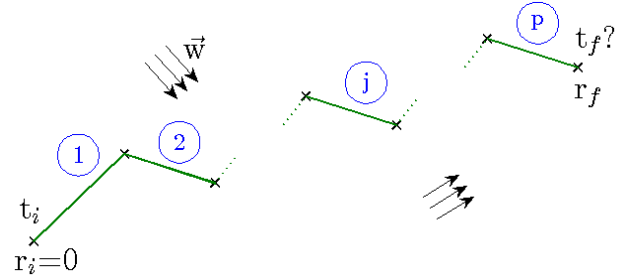


Figure 4. Sketch of a multi-segment cruise.

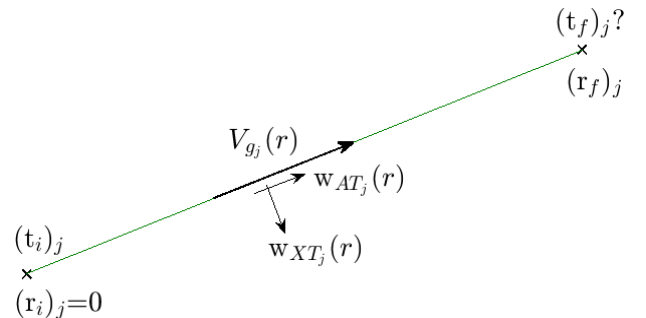


Figure 5. Sketch of a generic cruise segment.

The kinematic equation of motion for cruise flight, for segment  $j$ , can be written as (see [14]):

$$\frac{dt}{dr} = \frac{1}{V_{g_j}(r)}. \quad (4)$$

The time to fly the segment  $j$ , namely  $(\Delta t)_j$ , is obtained from the numerical integration of Eq. (4). In this work, the length of each cruise segment  $(r_f)_j$  and the initial time  $(t_i)_1 = t_i$  are given, and the continuity of the flight time enforces that  $(t_i)_j = (t_f)_{j-1}$ ,  $2 \leq j \leq p$ . Therefore, for each cruise segment, Eq. (4) is to be solved from  $r = 0$ , with initial condition  $t(0) = (t_i)_j$ , to the given length of the segment,  $r = (r_f)_j$ , which provides  $(t_f)_j = t((r_f)_j)$ , and then  $(\Delta t)_j = (t_f)_j - (t_i)_j$ .

Adding the solutions for all cruise segments, one can easily obtain the total flight time  $t_f$  given by

$$t_f = \sum_{j=1}^p (\Delta t)_j. \quad (5)$$

#### D. Ensemble trajectory prediction

Ensemble trajectory prediction is one of the main approaches commonly used for trajectory prediction subject to uncertainty provided by an EPS, as described in [11, 15]. In this approach, for each member of the ensemble, a deterministic trajectory predictor (TP) is used, leading to an ensemble of trajectories from which probability distributions can be derived.

In particular, for the ensemble member  $k$ , the procedure described in Section II.C for the computation of the flight time can be applied, obtaining  $t_f^{[k]}$  from the time to fly the segments, namely  $(\Delta t)_j^{[k]}$ ,  $1 \leq j \leq p$ . Therefore, for a given cruise path compatible with the airspace structure, the final result is a set of flight times  $(t_f^{[1]}, \dots, t_f^{[n]})$ , where  $n$  is the number of weather ensemble members. Moreover, this set can be statistically characterised by defining the mean and some quantification of the spread, such as the difference between the maximum and the minimum values.

#### E. Methodology for stochastic optimal path planning

Because the cruise flight is composed of several segments connecting given waypoints (including the origin and the destination), the aircraft route can be seen as a path in a graph. Therefore, the optimisation of the aircraft route with respect to a given objective function becomes a shortest path problem in

the sense of graph theory, which is defined by a set of  $m$  nodes (the waypoints), a set of  $l$  links (the constant-course segments) and a set of link costs (the increments of the objective function experienced at the segments).

However, as the problem is affected by uncertainty, it is indeed a stochastic shortest path problem. According to Gabrel et al. [16], when the uncertainty is not described by a probability distribution, it can be described with a model based on a discrete set of scenarios or with an interval model. In this work, the model based on a discrete set of scenarios is considered; each scenario is characterised by different wind and temperature fields, as defined by an ensemble member; and all the possible scenarios are taken into account in the optimisation. The problem is stated as selecting the unique route to be followed that minimises some function of the possible realisations of a given objective.

In this work, the stochastic approach is applied to find the route that minimises a combination of the average value of the total flight time (which is a good measure of the efficiency of the route) and a measurement of the spread of the trajectories, for instance, the difference between the largest flight time and the smallest one (which has an inverse relationship with the predictability); in this way, one can perform a trade-off between efficiency and predictability when addressing aircraft path planning. Hence, the following cost function is considered

$$J = \frac{1}{n} \sum_{k=1}^n t_f^{[k]} + dp \left[ \max_k(t_f^{[k]}) - \min_k(t_f^{[k]}) \right]. \quad (6)$$

where  $dp$  is the dispersion parameter, which controls the trade-off between efficiency and predictability; high values of  $dp$  lead to more predictable trajectories, but with larger average flight time (and, therefore, less efficient). Introducing the spread term in the objective function reduces the dispersion of the flight times; hence, the resulting route can be considered as a robust route, in the sense that it is highly efficient and yields similar values of the flight time for each weather scenario.

For time-invariant wind and temperature fields, the time to fly an allowed connection in the presence of every possible scenario does not depend on the time to reach the beginning of that connection; therefore, the times to fly all the possible connections under the weather scenario  $k$  can be a priori computed and stored in the vector  $c^{[k]}$  of length  $l$ . Assuming that the optimal path does not contain cycles, it can be characterised by a vector  $x$  of length  $l$  with binary components, which are either 1, if the corresponding segment belongs to the path, or 0 otherwise; thus,  $t_f^{[k]} = c^{[k]T} x$ . Furthermore, for a vector  $x$  to represent an admissible path, its non-zero components must correspond to a set of links connecting the origin to the destination without any interruption. To state this constraint, let  $A_{eq}$  be the node-arcs



incidence matrix of the graph, i.e., an  $m \times l$  matrix, whose  $i, j$ -component is 1 if the segment  $j$  begins with node  $i$ , -1 if segment  $j$  ends at node  $i$ , or 0 otherwise. Let also  $d$  be a vector of length  $m$ , whose components take the values 1, -1 or 0, depending on whether the corresponding node is the origin, the destination, or any other one, respectively. Then,  $x$  must satisfy  $A_{eq}x = d$ .

The optimal path planning problem can be formulated according to a combinatorial optimisation approach (as in [16]). Let  $\hat{c} = \frac{1}{n} \sum_{k=1}^n c^{[k]}$  be a vector containing the average value (among the weather scenarios) of the time to fly each segment; then, the problem of finding the path that minimises the objective in Eq. (4) can be formulated as a Mixed-Integer Linear Programming (MILP) problem as follows:

$$\left\{ \begin{array}{l} \min_{x,y,z} \quad \hat{c}^T x + dp (y - z) \\ \text{s.t.} \quad A_{eq} x = d \\ \quad y \geq c^{[k]T} x \quad \forall k \in \{1, \dots, n\} \\ \quad z \leq c^{[k]T} x \quad \forall k \in \{1, \dots, n\} \\ \quad x = \{0, 1\}^l \\ \quad y \in \mathbb{R}, \quad z \in \mathbb{R} \end{array} \right. \quad (7)$$

where  $y$  and  $z$  are real-valued, auxiliary decision variables, introduced to maintain the linearity of the cost function.

The methodology proposed in this paper is based on the application of GUROBI's MILP solver within a MATLAB interface. This solver implements a linear-programming based branch-and-bound algorithm, along with additional features such as pre-solving tasks, the addition of cutting planes, the application of heuristics to provide feasible solutions, and parellisation.

### III. RESULTS

In this section, the application considered in the paper is defined and the results are presented. In this work, Philadelphia International Airport (KPHL) and Barcelona–El Prat Airport (LEBL) have been selected as origin-destination pair, leading to a trans-oceanic route commonly flown. Both eastbound and westbound optimal routes are analysed. The coordinates of the airports are included in Table 1.

TABLE I. COORDINATES OF DEPARTURE AND ARRIVAL AIRPORTS

	<i>KPHL</i>	<i>LEBL</i>
Latitude	39° 52.2' N	41° 17.8' N
Longitude	75° 14.7' W	2° 4.7' E

ECMWF EPS has been chosen. The weather forecast have been retrieved from the TIGGE dataset, available at ECMWF portal. It was released 1 March 2017 at 00:00 with a look-ahead time of 24 hours, and it corresponds to a pressure altitude 200 hPa. The retrieval area goes from  $\phi_{\min} = 0^\circ$  to  $\phi_{\max} = 60^\circ$  N, and from  $\lambda_{\min} = 120^\circ$  W to  $\lambda_{\max} = 30^\circ$  E, with a retrieval step of  $0.25^\circ$  in latitude and longitude. The tuning parameter for the search area is set to  $k = 0.08$ , and the steps in latitude and longitude are  $\delta_{lat} = 0.5^\circ$  and  $\delta_{lon} = 2^\circ$ , respectively; it leads to  $m = 2060$  nodes and  $l = 49398$  links. In the following, results are presented for a cruise flight performed at Mach number  $M = 0.82$ , at a pressure altitude  $p = 200$  hPa ( $h = 11784$  m in the International Standard Atmosphere, which is in the stratosphere), and departing 1 March 2017 at 20:00h. The computational time spent to obtain the vectors and matrices involved in Eq. (7) has been around 14 s, whereas the elapsed time to obtain a solution has been under 370 s in all cases. The computations have been performed using a PC with an Intel Core i7-6700, under a Windows 10 operating system.

The optimal east- and westbound routes are presented in Fig. 6, for several values of  $dp$  (0, 3 and 6, for the eastbound flight, and 0, 0.6 and 4, for the westbound flight) along with the route of minimum distance as a reference, a representative wind field (the average along the EPS members), and the wind uncertainty field, which is defined as the square root of the sum of the zonal wind variance,  $\sigma_u^2$ , and the meridional wind variance,  $\sigma_v^2$ . For this weather forecast and for  $dp = 0$ , one can see that the route from KPHL to LEBL (blue solid line in Fig. 6) is somehow shifted to the south, in order to take more advantage of the predominant tailwinds, whereas the route from LEBL to KPHL (blue dashed line in Fig. 6) is deviated far to the north, to avoid encountering strong headwinds. Nevertheless, both routes cross areas with higher wind uncertainty (with a darker background colour in Fig. 6); these areas cover the northeast coast of North America, including Philadelphia Airport, and have their epicentre off the south coast of Nova Scotia. Therefore, as  $dp$  increases, the trajectories (both eastbound and westbound) are deviated to the north in order to avoid these areas with higher wind uncertainty, and to spend more time within areas with lower wind uncertainty (with a lighter background colour in Fig. 6); the higher the  $dp$  value considered, the larger the deviations with respect to the optimal route for  $dp = 0$ .

The values of the optimal total flight time corresponding to these trajectories are presented in Table 2. The average  $E[t_f]$  is computed along the EPS members, and the spread  $\Delta[t_f]$  is defined as the difference between the largest value and the smallest one. Note that  $E[t_f] + dp \Delta[t_f]$  is the minimum value of  $J$ .

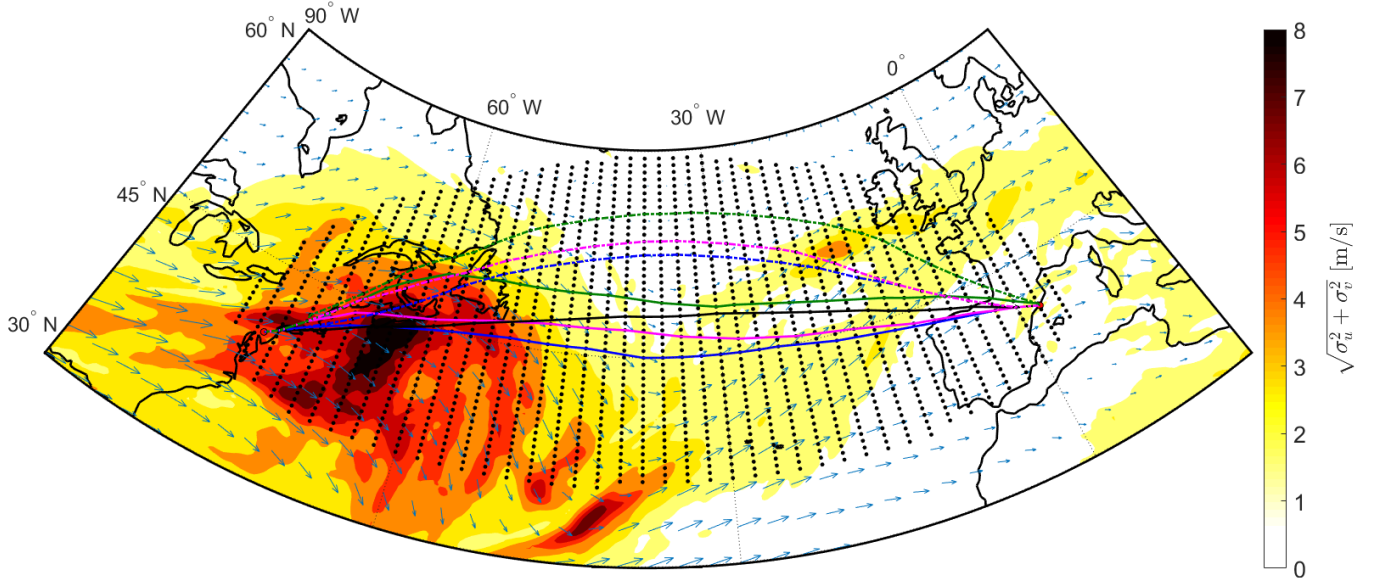


Figure 6. Optimal routes from KPHL to LEBL:  $dp = 0$  (blue solid),  $dp = 3$  (magenta solid), and  $dp = 6$  (green solid); optimal routes from LEBL to KPHL:  $dp = 0$  (blue dashed),  $dp = 0.6$  (magenta dashed), and  $dp = 4$  (green dashed); route of minimum distance (black); average wind field (blue arrows). Background: wind uncertainty field.

TABLE II. AVERAGE VALUE AND SPREAD OF THE TOTAL FLIGHT TIME FOR EASTBOUND AND WESTBOUND OPTIMAL TRAJECTORIES, AND FOR DIFFERENT VALUES OF  $dp$

$dp$	KPHL to LEBL			LEBL to KPHL		
	0	3	6	0	0.6	4
$E[t_f]$ , min	383.09	384.61	391.58	502.03	503.02	504.27
$\Delta[t_f]$ , min	5.60	4.47	3.00	11.41	8.28	6.97

First, these results show that for the westbound optimised cruise one has larger values of the mean than for the eastbound optimised cruise (as expected, because in the latter case one can take advantage of the jet stream), and also larger values of the spread.

As previously mentioned, the stochastic optimal path planning is not only capable of providing more efficient and more predictable trajectories, but also it allows one to perform a trade-off analysis between efficiency and predictability. Results of this analysis show, as expected, that the higher the value of  $dp$ , the lower the dispersion in the total flight time, but the higher the average total flight time. In particular, for  $dp = 3$  as compared to  $dp = 0$ , one can have a decrease of 1.13 min in  $\Delta[t_f]$  (that is, 20%) at a cost of an increase of 1.52 min in  $E[t_f]$  (that is, 0.40%) when

flying from KPHL to LEBL. Analogously, for  $dp = 0.6$  as compared to  $dp = 0$ , one can have a decrease of 3.13 min in  $\Delta[t_f]$  (that is, 27%) at a cost of an increase of 0.99 min in  $E[t_f]$  (that is, 0.20%) when flying from LEBL to KPHL. In both cases, for the weather forecast considered, a substantial gain in predictability can be achieved at a very low cost in terms of efficiency, just by choosing an appropriate route.

From a multi-objective optimisation point of view, the optimal pair of values  $(E[t_f], \Delta[t_f])$  obtained for different values of  $dp$  describe a curve that can be interpreted as the Pareto frontier corresponding to the conflicting objectives  $E[t_f]$  and  $\Delta[t_f]$ . The aircraft paths that lead to the pair of values  $(E[t_f], \Delta[t_f])$  are Pareto optimal because no other path can improve neither of the objectives without degrading the other one. In Fig. 7, the Pareto frontiers for eastbound and westbound trajectories are depicted; they have been restricted to an interval of  $dp$  ranging from 0 to 10, and the values corresponding to the optimal routes shown in Fig. 6 are also depicted as coloured dots. These curves are very useful to present the results of the optimisation to the Airspace Users (AUs) in a clear and condensed form, and have the main advantage that the AUs can make a decision without revealing their cost structure.

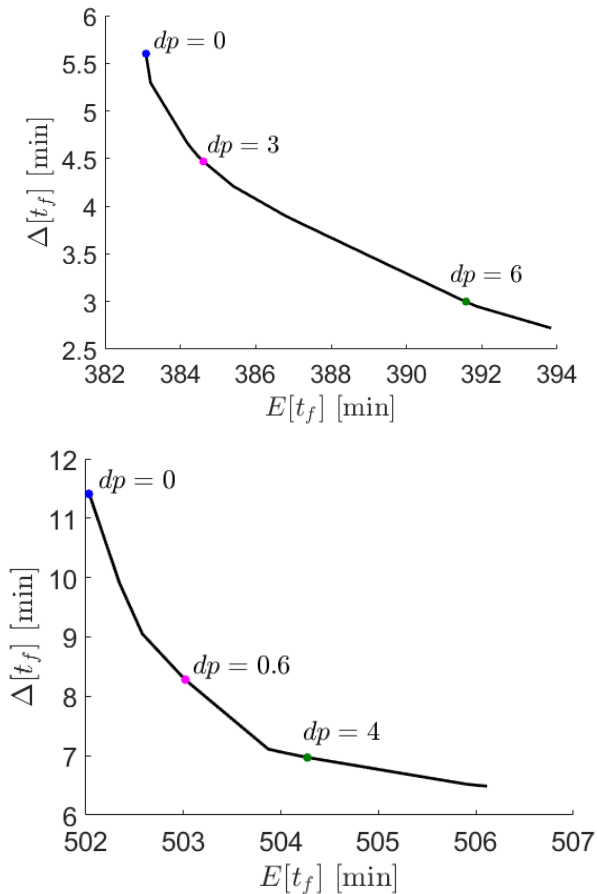


Figure 7. Trade-off analysis between efficiency and predictability. Eastbound trajectory (top), westbound trajectory (bottom).

#### IV. FINAL REMARKS

The general framework for this paper is the development of a methodology to manage weather uncertainty suitable to be integrated into the trajectory planning process. In particular, a stochastic methodology has been implemented, which is capable of finding the optimal aircraft path, considering a structured airspace, in the presence of uncertain winds and uncertain temperature provided by an EPS. Furthermore, the advantages of applying this methodology to obtain efficient and more predictable routes have been quantified, which show that, for certain weather forecasts, important enhancements in predictability can be achieved with a very low impact on efficiency. It is noteworthy that the advantages of the approach strongly depend on the weather affecting the flight.

The extension of this methodology to consider a time-dependent wind field is left for future work. The main associated change is that the time to fly a cruise segment under a time-variant wind scenario depends on the time to reach the beginning of the segment. Thus, the time to fly a path under any scenario is no longer linear on vector  $x$ , which leads to a non-linear cost function and non-linear

inequality constraints. The problem would become a Mixed-Integer Non-Linear Programming (MINLP) problem, which increases its complexity.

#### ACKNOWLEDGMENT

The authors gratefully acknowledge the financial support of the Spanish Ministerio de Economía y Competitividad through grant TRA2014-58413-C2-1-R, co-financed with FEDER funds.

#### REFERENCES

- [1] Nilim, A., L. El Ghaoui, M. Hansen, and V. Duong. 2001. "Trajectory-based air traffic management (TB-ATM) under weather uncertainty," 4th USA-Europe ATM Seminar (ATM2001). 1–11.
- [2] Grabbe, S., B. Sridhar, and A. Mukherjee. 2009. "Sequential traffic flow optimization with tactical flight control heuristics," *Journal of Guidance, Control and Dynamics*. 32 (3): 810–820.
- [3] Sauer, M., T. Hauf, and C. Forster. 2014. "Uncertainty Analysis of Thunderstorm Nowcasts for Utilization in Aircraft Routing," 4th SESAR Innovation Days (SID2014). 1–8.
- [4] Girardet, B., L. Lapasset, D. Delahaye, and C. Rabut. 2014. "Wind-optimal path planning: Application to aircraft trajectories," 13th International Conference on Control Automation Robotics & Vision (ICARCV2014). 1403–1408.
- [5] González-Arribas, D., M. Soler, and M. Sanjurjo-Rivo. 2018. "Robust Trajectory Planning Under Wind Uncertainty Using Optimal Control," *Journal of Guidance Control and Dynamics*. 41 (3): 673–688.
- [6] Rosenow, J., Strunck, D., and H. Fricke, 2018. "Trajectory Optimization in Daily Operations," 8th International Conference for Research in Air Transportation (ICRAT2018). 1–8.
- [7] AMS. 2008. "Enhancing Weather Information with Probability Forecasts," *Bull Amer. Meteor. Soc.* 89.
- [8] Arribas, A., K.B. Robertson, and K.R. Mylne. 2005. "Test of a poor man's ensemble prediction system for short-range probability forecasting," *Monthly Weather Review*. 133 (7): 1825–1839.
- [9] Lu, C., H. Yuan, B.E. Schwartz, and S.G. Benjamin. 2007. "Short-range numerical weather prediction using time-lagged ensembles," *Weather and Forecasting*. 22 (3): 580–595.
- [10] Steiner, M., C.K. Mueller, G. Davidson, and J.A. Krozel. 2008. "Integration of probabilistic weather information with air traffic management decision support tools: a conceptual vision for the future," 13th Conference on Aviation, Range and Aerospace Meteorology. 1–9.
- [11] Cheung, J., A. Hally, J. Heijstek, A. Marsman, and J.-L. Brenguier. 2015. "Recommendations on trajectory selection in flight planning based on weather uncertainty," 5th SESAR Innovation Days (SID2015). 1–8.
- [12] Steiner, M., R. Bateman, D. Megenhardt, Y. Liu, M. Xu, M. Pocerich, and J.A. Krozel. 2010. "Translation of ensemble weather forecasts into probabilistic air traffic capacity impact," *Air Traffic Control Quarterly*. 18 (3): 229–254.
- [13] Dancila, B. D., and R. M. Botez. 2016. "Geographic Area Selection and Construction of a Corresponding Routing Grid Used for in-Flight Management System flight trajectory optimization," *Institution of Mechanical Engineers, Part G: Journal of Aerospace Engineering*, 231 (5): 809–822.
- [14] Vinh, N. 1993. *Flight Mechanics of High-Performance Aircraft*. Cambridge University Press, New York. 112.
- [15] Cheung, J., J.-L. Brenguier, J. Heijstek, A. Marsman, and H. Wells. 2014. "Sensitivity of flight durations to uncertainties in numerical weather predictions," 4th SESAR Innovation Days (SID2014). 1–8.
- [16] Gabrel, V., C. Murat, and L. Wu. 2013. "New models for the robust shortest path problem: complexity, resolution and generalization," *Annals of Operations Research*. 207 (1): 97–120.